Magnetic Characterization of Magnetite Particles for MR Contrast Agents

Motoshi Suzuki, Wataru Shimizu, Yoshio Kosugi,† Hiroyuki Honda, and Takeshi Kobayashi*

Department of Biotechnology, Faculty of Engineering, Nagoya University, Furo-cho, Chikusa-ku, Nagoya 464-01

†Department of Applied Chemistry, Faculty of Engineering, Nagoya University, Furo-cho, Chikusa-ku, Nagoya 464-01

(Received November 21, 1995)

The proton spin relaxivities (*R1*, *R2*) of agarose phantom with magnetite particles were measured using an NMR spectrometer at 5.875 T, and compared with other magnetic substances. *R2* for the polyethylene glycol-coated magnetite particle (PEG-magnetite) was 455 s^{-1} mM^{-1} (M=mol dm^{-3}), 50- and 95-times larger than that for $FeCl_3$ and Gd(H_2dtpa), respectively. PEG-magnetite also showed a high *R2*/*R1* ratio of 172, while the latter two substances had low *R2*/*R1* ratios below 10. The core size greatly affected *R2*, the maximum *R2* value being observed in the case of the intermediate size (10 nm) among three different core sizes of magnetite. The basic characteristics of magnetite were found to be derived from its magnetism. The optimization of such acquisition parameters as *TR* and *TE* for spin-echo pulse sequences was also examined. The differences in the calculated signal intensity obtained from a tumor with PEG-magnetite and from normal tissue without PEG-magnetite were compared. The image with the highest contrast was found to be obtained at *TE* = 40 ms and an appropriately long *TR*. PEG-magnetite is expected to work well as a negative-contrast agent under suitable acquisition conditions.

Along with the development of MRI techniques, the effects of materials which can enhance tissue contrast have also been investigated. These materials are classified into positive and negative MR contrast agents. Positive contrast agents mainly shorten *T1* and increase the signal intensity, while negative agents mainly shorten *T2* and decrease the signal intensity. One type of positive contrast agent, paramagnetic metal-ion chelates, has been well studied, and are employed in clinical diagnosis in some areas. For example, gadolinium *N*,*N*′,*N*′,*N*″,*N*″-diethylenetriaminepentaacetate [Gd(H_2dtpa)] is now widely used in MRI of the central nervous system. However, more extensive use of these positive contrast agents has been limited by their inherent properties that affect their distribution to tissues. Small particles of ferromagnetic substances can function as negative contrast agents. Important targets in organ systems are not only the reticuloendothelial system, but also the gastrointestinal tract[1] and blood-pool compartments;[2] an interesting approach to these targets is the target-directing of magnetic particles in order to deliver them to a particular tissue via receptor-binding molecules or monoclonal antibodies.

We have established a method for preparing antibody-conjugated magnetite particles.[3] When a monoclonal antibody against a cancer-associated antigen was conjugated with polyethylene glycol-coated magnetite particles (PEG–magnetite), the particles were found to accumulate specifically in the tumor tissue and to cause a change in the MR signal intensity,[4] thus showing the effectiveness of antibody-conjugated magnetite particles as an MR contrast agent for cancer diagnosis. The efficiency in proton relaxation as well as appropriate biodistribution are needed for the employment of such particles as an MR contrast agent. In the present study, the longitudinal and transverse relaxivities of PEG–magnetite were measured and compared with the values for other magnetite particles and metal ions. Additionally, magnetite particles of three different sizes were prepared, and their relaxivities and other magnetic parameters derived from their magnetization curves were compared. Suitable acquisition parameters for PEG–magnetite were also examined.

Materials and Methods

Test Substances. Polyethylene glycol-coated and oleic acid-coated magnetite particles (PEG–magnetite and OA–magnetite) were the magnetic particles used. PEG–magnetite was prepared by the co-precipitation method in a polyethylene glycol solution, as reported previously.[3] OA–magnetite was prepared from a magnetite core coated with oleic acid so as to disperse in water.[5] The core size of the OA–magnetite varied with the concentration of $NaNO_2$ at the time of co-precipitation.[6] A commercially available water-based ferrofluid, Marpomagna® FW-40 (Matsumoto Yushi-Seiyaku Co., Osaka, Japan), was also used as a magnetic-particle control substance. The overall sizes of the particles of these three substances were measured by a dynamic light-scattering system (DLS-700, Ohtsuka Electronics Co., Osaka, Japan), and the core sizes by a transmission electron microscope (H-800, Hitachi Co., Tokyo, Japan). The particle and core sizes are given in Table 1.

Iron(III) chloride ($FeCl_3$) and Gd(H_2dtpa) were used as non-particulate control substances. Analytical-grade iron(III) chloride (Wako Pure Chemical Industries, Co., Osaka, Japan) was used without purification. A pharmaceutical form of Gd(H_2dtpa) (Magnevist®) was kindly provided by Nihon Schering Co. (Osaka,

Table 1. Core and Particle Sizes of Magnetic Particles of Three Different Substances

Test substance (Code#)	Core size	Particle size
	nm	nm
PEG–magnetite	ca. 5	147
Marpomagna®	ca. 10	82.5
OA–magnetite (#05)	ca. 5	60.2
(#10)	ca. 10	78.3
(#35)	ca. 35	78.9

Japan). This was supplied in an ampul as an aqueous solution with a concentration of 0.5 mol-Gd/dm^{-3}, and was used without further treatment.

Various concentrations of the test substances were dispersed in 0.5% agarose gel phantom (tissue imitation material). A uniform distribution of the particulate substances was attained by mixing them into an agarose solution just prior to gelification of the agarose. The other test substances, iron(III) chloride and Gd(H_2dtpa), were also homogeneously dispersed in the agarose gel. All measurements of the magnetic properties were performed using these agarose phantoms.

The iron concentration of the agarose phantom with magnetic particles was determined spectrophotometrically[7] as follows. Agarose gel containing magnetic particles was completely dissolved in excess HCl, after which the solution was oxidized with H_2O_2 and mixed with KSCN solution. The absorbance of the thiocyanato-iron(III) complex at 480 nm was then measured. The same method was employed for iron(III) chloride samples. For Gd(H_2dtpa), the gadolinium concentration in the agarose phantom with Gd(H_2dtpa) was calculated based on the degree of dilution from the Magnevist® ampul.

Relaxation Time Measurements. Samples for relaxation-time measurement were prepared in double-concentric NMR test tubes with a diameter of 5 mm. The outer tube was filled with a solvent for signal locking (deuterated chloroform, $CDCl_3$) together with a standard substance (1% tetramethylsilane). The agarose phantom (0—0.5 mmol-Fe or Gd/dm^3) was packed into the inner capillary tube.

Relaxation measurements were performed on a Bruker AC-250 NMR spectrometer equipped with an ASPECT 3000 system, operated at a magnetic flux density of 5.875 T. The 90° -pulse width was optimized for each sample. The longitudinal relaxation time (*T1*) was obtained from an inversion recovery sequence. The transverse relaxation time (*T2*) was derived from a Carr–Purcell–Meiboom–Gill sequence. Four samples of different concentrations were used and the longitudinal relaxivity (*R1*) and the transverse relaxivity (*R2*) were determined form plots of the relaxation rates (1/*T1* and 1/*T2*) against the concentration of the contrast agent (*C*) according to following equations:

$$\frac{1}{T1} = \frac{1}{T1_0} + R1 \cdot C \quad (1)$$

and

$$\frac{1}{T2} = \frac{1}{T2_0} + R2 \cdot C, \quad (2)$$

where $T1_0$ and $T2_0$ are the substance's intrinsic relaxation times.

Magnetization Measurement. Magnetization curves of agarose phantom samples with OA–magnetite were obtained using a vibrating sample magnetometer (Model VSM-5; Toei Kogyo Co., Tokyo, Japan). The agarose phantom (iron content, 0.1 mol-Fe/dm^3) was packed in a cylindrical sample cell made of acrylic resin (5 mm inner diameter, 8 mm inner height). After the sample had been centered on the magnet coil of the apparatus, the magnetization was recorded as the intensity of the magnetic field was changed.

Results and Discussion

Relaxivities of Magnetic Materials. The relaxation rates of agarose phantoms with PEG-magnetite, Marpomagna®, iron(III) chloride and Gd(H_2dtpa) are shown in Fig. 1(a) and (b) for various concentrations of iron or gadolinium. A linear dependence of 1/*T1* and 1/*T2* on the metal-atom concentration was observed for all of the test substances. The relaxivities of these four substances were calculated and are given in Table 2. The relaxivities (*R1* and *R2*) indicate the degree of concentration-dependence; a contrast agent with a large relaxivity can work at a low concentration, and only a low dose is needed. The ratio *R2/R1* is an indicator of the efficiency of negative contrast agents. Therefore, *R2* and the *R2/R1* ratio are important parameters in evaluating the magnetic particles for use as MR contrast agents.

Large differences in *R2* were observed among the substances tested, with the particulate substances showing higher *R2* values than the ionic ones. PEG–magnetite had an *R2* value per mole of metal atoms about 50-times larger than that of $FeCl_3$ and about 95-times larger than that of Gd(H_2dtpa). Josephson et al.[8] studied the relaxivities of superparamagnetic iron oxide particles and paramagnetic ion chelates and reported a similar tendency.

The test substances were classified into two groups according to their *R2/R1* ratio; the ionic substances had low *R2/R1* ratios below 10, while the particulate substances had high ratios above 170. This means that the effect of these particulate substances on *T2* is much stronger than on *T1*, and that they can therefore be good negative contrast agents. Rogers et al.[9] reported similar results at a magnetic field intensity of 2 T; the *R2/R1* ratios for Gd(H_2dtpa) and for one of the superparamagnetic iron oxide particles were 1.06 and 179, respectively. Josephson et al.[8] pointed out that a product with an *R2/R1* ratio above 25 at a magnetic-field intensity

Table 2. Relaxivities of Various Magnetic Substances

Test substance (Code#)	*R1*[a]	*R2*[a]	*R2*/*R1*
	$s^{-1}mM^{-1}$	$s^{-1}mM^{-1}$	—
PEG–magnetite	2.63	466	177
Marpomagna®	0.963	359	373
$FeCl_3$	1.38	9.25	6.70
Gd(H_2dtpa)	4.09	4.77	1.17
OA–magnetite (#05)	1.61	443	275
(#10)	1.24	622	502
(#35)	1.28	536	419

a) mM is the millimolar concentration of metal atoms (iron or gadolinium).

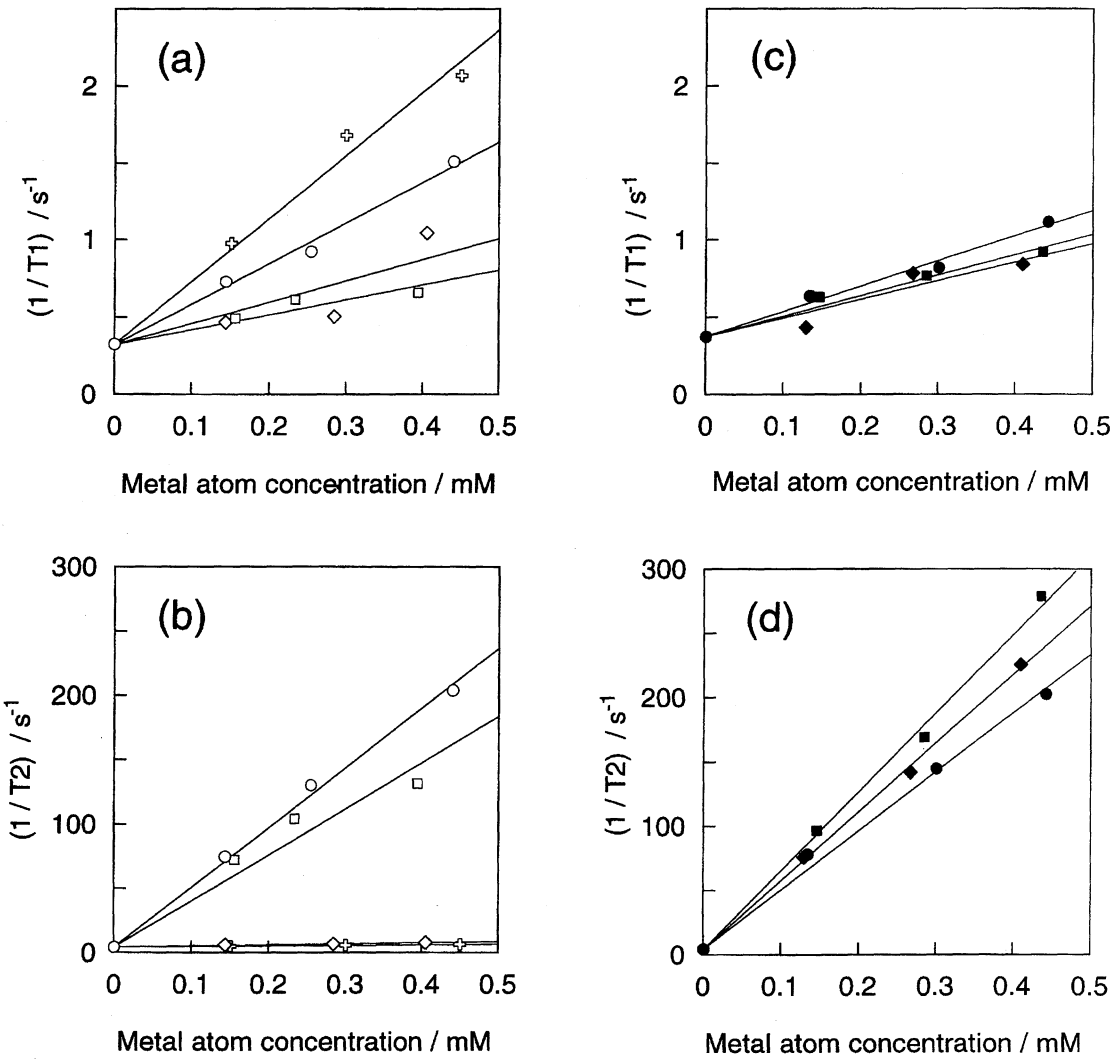

Fig. 1. Relaxation rates as a function of metal atom concentration in agarose phantom with various magnetic substances. (a) and (c): longitudinal relaxation rate; (b) and (d): transverse relaxation rate. PEG–magnetite (○), Marpomagna® (□), iron(III) chloride (◇), Gd(H_2dtpa) (✣), and OA–magneite #05 (●), #10 (■), #35 (◆).

of 0.47 T was either a ferromagnetic or superparamagnetic iron oxide whose clustered structure limited the contact between iron oxide crystals and water. PEG–magnetite and Marpomagna® are thought to have a high iron content that limits the contact between the iron oxide crystals and water, resulting in a high *R2*/*R1* ratio.

Marpomagna® was found to have a larger *R2*/*R1* ratio than PEG–magnetite, but does not have functional groups for linkage on the surface. Since PEG–magnetite can be linked with an antibody, it is suitable as a negative-contrast agent.

It is considered that the relaxivities of a particulate magnetic material, such as PEG–magnetite, depends on its physicochemical structure. The magnetite core can change from a ferromagnetic to a superparamagnetic form as the size decreases. Thus, to elucidate the characteristics of PEG–magnetite, OA–magnetites with three different core sizes were prepared and their relaxivities were measured together with the dependence of the relaxivities on core size.

Dependence of OA–Magnetite Relaxivities on Core Size. The relaxivities were obtained for agarose phantoms containing OA–magnetites with three different sizes. The relationships between the iron concentration and relaxation rates (1/*T1* and 1/*T2*) are shown in Fig. 1(c) and (d). The calculated relaxivities (Table 2) show that the core size of the magnetite significantly affects *R2*, though an increase in the core size does not always result in a higher *R2* value: The highest *R2* value was observed in the case of the intermediate core size (code #10). Josephson et al.[8] reported that the superparamagnetic form of iron oxide has high relaxivities (both *R1* and *R2*) compared with the ferromagnetic form. Therefore, in order to explain the relationship between the relaxivity and the core size we examined the magnetism and other magnetic properties of the OA–magnetites.

The magnetization of each agarose phantom was recorded against the magnetic-field intensities between −800 and +800 kA m^{-1}, and are shown in Fig. 2(a). For all of the substances, the magnetization reached 90% of saturation at 100 kA m^{-1}, and then gradually increased up to saturation. All of the curves exhibited very narrow hysteresis loops, sug-

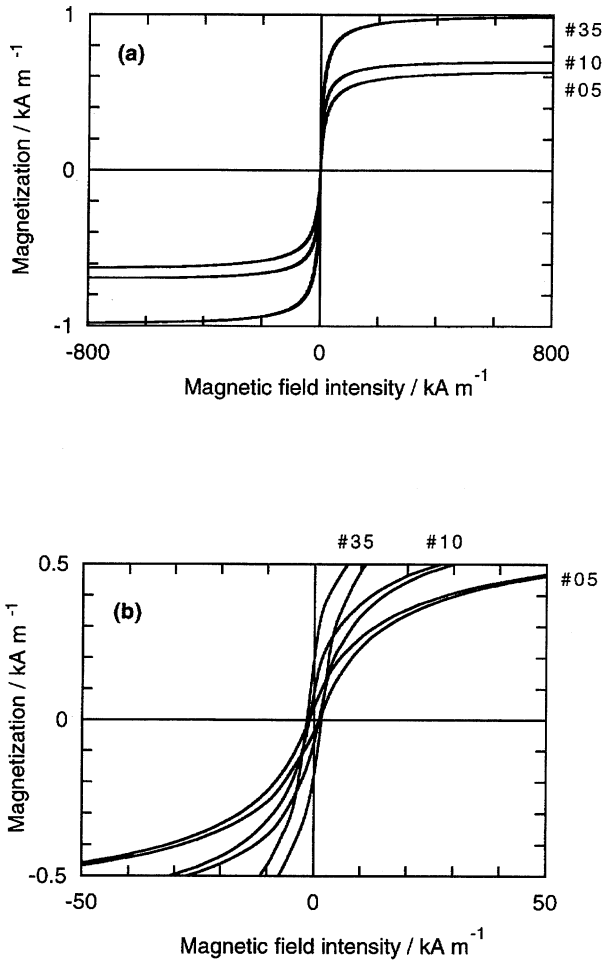

Fig. 2. Magnetization curves of agarose phantom with OA–magnetite. The iron content was 0.1 mol-Fe/dm^3. OA–magnetite code numbers are shown on the upper right.

gesting that the substances are like superparamagnetic materials, as reported by Bean.[10] In order to clarify the difference in the three OA–magnetites, the curve profiles between ±50 kA m^{-1} were plotted, and are shown in Fig. 2(b).

Magnetic properties, such as saturation magnetization, residual magnetization, and coercive force, were evaluated from the magnetization curves. The initial susceptibility and hysteresis loss were calculated from the slope of the curve at zero field and the area surrounded by the curve, respectively. These values are given in Table 3. Most of the magnetic properties derived from the magnetization curves increased along with an increase in the core size. However, the coercive force and hysteresis loss of OA–magnetite #05 and #10 were almost the same, and smaller than those of #35. The initial susceptibility appears to be related to the core size, including the size distribution, and could therefore be a substitutable parameter for the core size. The coercive force is a parameter that can explain the delicate differences in magnetism.[10]

Pouliquen et al.[11] measured the relaxivities and susceptibilities of six dextran–magnetites with various core sizes below 25 nm, and demonstrated that there is a linear correlation between their susceptibilities and *R2/R1* ratios. Figure 3 shows the relationship between susceptibility and *R2/R1* ratio and between the susceptibility and coercive force for the OA–magnetites. OA–magnetites #05 and #10 possessed very little coercive force, while a linear relationship was obtained between their susceptibilities and *R2/R1* ratios, which is in agreement with that of Pouliquen et al. OA–magnetite #35 was found to possess much greater coercive force than the other two. These results indicate that OA–magnetites #05 and #10 are superparamagnetic materials, while OA–magnetite #35 is not. Thus, the relationship between *R2/R1* and the susceptibility can be explained by the difference in the magnetic behavior.

Table 3. Magnetic Properties of OA–Magnetite with Different Core Sizes[a)]

Code size	M_s	M_r	H_c	χ_i	W_h
nm	kA m^{-1}	kA m^{-1}	kA m^{-1}	—	J m^{-3}
5	0.628	0.0379	1.11	0.0363	0.0288
10	0.694	0.0702	1.09	0.0657	0.0344
35	0.980	0.194	1.56	0.125	0.0671

a) M_s: saturation magnetization, M_r: residual magnetization, H_c: coercive force, χ_i: initial susceptibility, W_h: hysteresis loss.

Estimation of Change in MR Signal Intensity Due to PEG–Magnetite. Since relaxivities *R1* and *R2* are indicators of the effectiveness of MR contrast agents, the change in the MR signal can be estimated from these values. For a spin-echo pulse sequence with a repetition time of *TR* and echo time of *TE*, the signal intensity (*S*) is calculated as follows:[12]

$$S = k \cdot e^{-\frac{TE}{T2}} \cdot \left\{1 - e^{-\frac{TR}{T1}} \cdot \left(2 \cdot e^{\frac{TE}{2 \cdot T1}} - 1\right)\right\}, \quad (3)$$

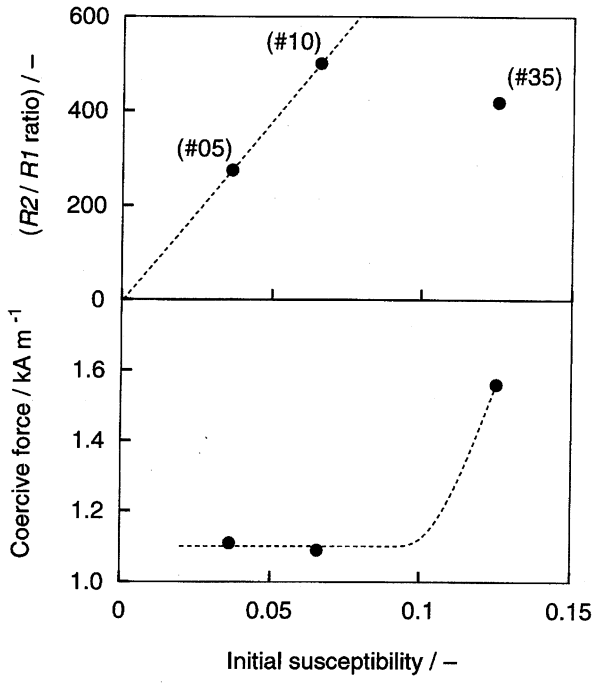

Fig. 3. Relationship between *R2/R1* and initial susceptibility, and between coercive force and initial susceptibility.

where k is a variable parameter including the proton density, but is assumed to be a constant in the present case. It is known that the signal intensity calculated from Eq. 3 fits well with the actual MR signal intensities.[9] By this means, the concentration-dependency of PEG–magnetite and pulse sequence optimization was examined.

The signal intensity was calculated as a function of the PEG–magnetite concentration for three spin-echo pulse sequences. As representative values of *T1*-weighted (short *TR*/short *TE*), proton density-weighted (long *TR*/short *TE*), and *T2*-weighted (long *TR*/long *TE*) sequences, *TR*/*TE*=400/20, 1500/20, and 1500/80 were used, respectively. The values of *T1* and *T2* at any concentration were determined from Eqs. 1 and 2 using the intrinsic relaxation times $T1_0$=2850 ms and $T2_0$=235 ms, which correspond to the conditions for 0.5% agarose at 5.875 T and the relaxivities *R1* and *R2* of PEG–magnetite shown in Table 2. The calculated signal intensities were normalized to the value for C=0, and are plotted in Fig. 4. The signal intensity decreased with increasing the concentration in all cases, but especially in the *T2*-weighted sequence. The concentration at which the signal intensity decreased to half was 20 μmol-Fe/dm^3 in the case of the *T2*-weighted sequence.

Many MR images can be acquired from one subject by changing the operator-selected acquisition parameters, such as *TR* and *TE*. In order to take advantage of a contrast agent at its maximum efficiency, it is important to acquire images at suitable acquisition parameters. We compared the difference in the MR signal intensities obtained from a tumor with PEG–magnetite and from normal tissue without PEG–magnetite using normal tissue phantom conditions[4] ($T1_0$=1180 ms and $T2_0$=15.7 ms). In an in vivo experiment performed previously,[4] a 50% decrease in the tumor MR signal intensity was observed at *TR*/*TE*=1500/60 when a cancer-specific monoclonal antibody-conjugated PEG–magnetite was administrated to a tumor-bearing mouse dosed with 100 μmol-Fe/kg-body weight. Therefore, a PEG-magnetite concentration (C) of 20 μmol-Fe/dm^3 was used in the calculation.

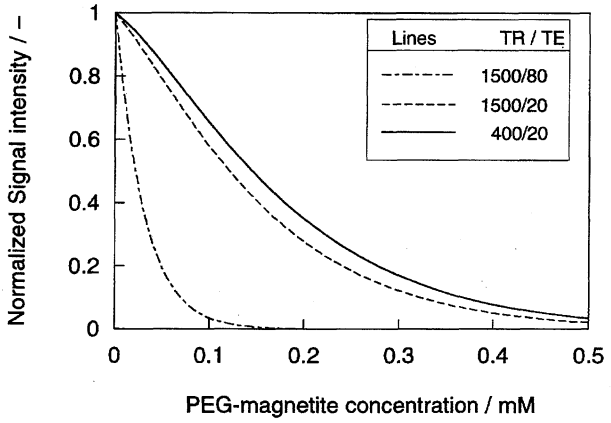

Fig. 4. Dependency of concentration of PEG–magnetite on MR signal intensity. The signal intensity was normalized to the value for C=0. The pulse sequence (*TR*/*TE*) is shown in the upper right corner.

Changing the parameters *TR* and *TE*, the signal intensities of normal tissue (S_{Normal}) and the tumor (S_{Tumor}) were calculated using Eqs. 1, 2, and 3 under the conditions C=0 and C=20 μmol-Fe/dm^3, respectively. In order to analyze the contrast quantitatively, a variable (ΔS) was introduced,

$$\Delta S = S_{Normal} - S_{Tumor}. \quad (4)$$

The profile of ΔS versus various values of *TR* and *TE* is shown in Fig. 5. A mountain-like shape with a ridge at *TE*=20 ms was obtained. A long *TR* resulted in a large ΔS, but also caused a long acquisition time. It was found that the image with the highest contrast could be taken with a *TE*=20 ms and an appropriately long *TR*, such as 1500 ms.

The pulse sequence was optimized not only for C=20 μmol-Fe/dm^3, but also for other concentrations (data not shown), since the PEG–magnetite will be distributed to other tumor tissue at different concentrations because of differences in the affinity between the tumor and the monoclonal antibody-conjugated PEG–magnetite. At concentrations higher than 20 μmol-Fe/dm^3, the largest ΔS was obtained at a *TE* shorter than 20 ms, whereas at a concentration lower than 20 μmol-Fe/dm^3, the largest ΔS was given with a *TE* longer than 20 ms. Since different tissues have different relaxation times, optimizations were also performed for other *T1* and *T2* values (data not shown). The pulse sequence *TR*/*TE* gave the largest ΔS changed in every case. This procedure to obtain the largest ΔS should thus be performed for various types of tissue in practical MRI applications.

In conclusion, we derived the magnetic characteristics of magnetite particles, and found the PEG–magnetite affects proton relaxation to a high degree. The maximum *R2* was observed with a core size of 10 nm. When used with suitable acquisition parameters, PEG–magnetite will work well as a negative-contrast agent.

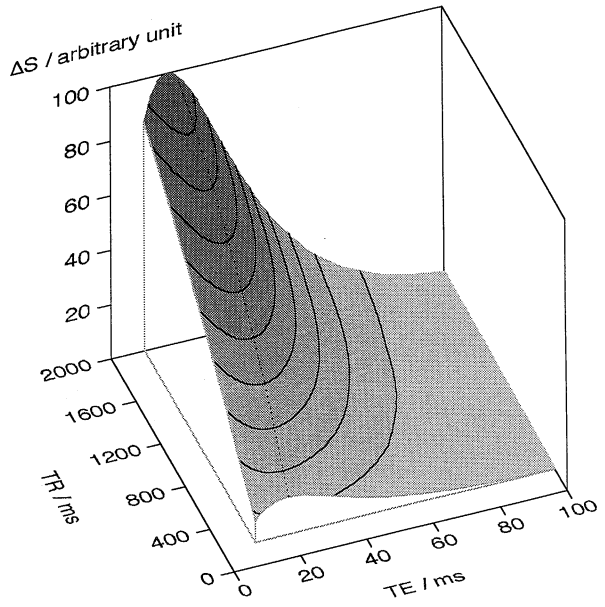

Fig. 5. Pulse sequence optimization. Values used in the calculation are given in the text.

The authors wish to thank Drs. Masaaki Matsui and Masaaki Doi (Faculty of Engineering, Nagoya University) for their assistance in VSM work, Dr. Yoshikazu Fujii (Faculty of Medicine, Nagoya University) for his help with electron microscopy, and Dr. Toyoko Imaei (Faculty of Science, Nagoya University) for assisting with dynamic light-scattering work. The authors also express their thanks Drs. Masaya Takahashi and Takashi Tsuji of Nihon Schering for kindly providing Magnevist®.

References

1) T. Bach-Gansmo, B. Dupas, M. Gayet-Delacroix, and M. Lambrechts, *Br. J. Radiol.*, **66**, 420 (1993).

2) T. A. Kent, M. J. Quast, B. J. Kaplan, R. S. Lifsey, and H. M. Eisenberg, *Magn. Reson. Med.*, **13**, 434 (1990).

3) M. Suzuki, M. Shinkai, M. Kamihira, T. Hanaichi, and T. Kobayashi, *Biotechnol. Appl. Biochem.*, **21**, 335 (1995).

4) M. Suzuki, H. Honda, T. Kobayashi, T. Wakabayashi, J. Yoshida, and M. Takahashi, *Brain Tumor Pathol.*, in press.

5) M. Shinkai, M. Suzuki, S. Iijima, and T. Kobayashi, *Biotechnol. Appl. Biochem.*, **21**, 125 (1994).

6) M. Shinkai, H. Honda, and T. Kobayashi, *Biocatalysis*, **5**, 61 (1991).

7) C. S. Owen and N. L. Sykes, *J. Immunol. Methods*, **73**, 41 (1984).

8) L. Josephson, J. Lewis, P. Jacobs, P. F. Hahn, and D. D. Stark, *Magn. Reson. Imaging*, **6**, 647 (1988).

9) J. Rogers, J. Lewis, and L. Josephson, *Magn. Reson. Imaging*, **12**, 631 (1994).

10) C. P. Bean, *J. Appl. Phys.*, **26**, 1381 (1955).

11) D. Pouliquen, H. Perroud, F. Calza, P. Jallet, and J. J. Le Jeune, *Magn. Reson. Med.*, **24**, 75 (1992).

12) P. B. Morris, "Nuclear Magnetic Resonance Imaging in Medicine and Biology," Clarendon Press, Oxford (1986).